

Antimony vibrations in skutterudites probed by ^{121}Sb nuclear inelastic scattering

H.-C. Wille,^{1,2,*} R. P. Hermann,^{3,4} I. Sergueev,¹ O. Leupold,² P. van der Linden,¹ B. C. Sales,⁵ F. Grandjean,³ Gary J. Long,⁶ R. Rüffer,¹ and Yu. V. Shvyd'ko⁷

¹European Synchrotron Radiation Facility, F-38043 Grenoble Cedex, France

²Hamburger Synchrotronstrahlungslabor, D-22607 Hamburg, Germany

³Department of Physics, B5, Université de Liège, B-4000 Sart-Tilman, Belgium

⁴Institut für Festkörperforschung, Forschungszentrum Jülich GmbH, D-52425 Jülich, Germany

⁵Solid State Division, Oak Ridge National Laboratory, Oak Ridge, Tennessee 37831, USA

⁶Department of Chemistry, University of Missouri–Rolla, Rolla, Missouri 65409-0010, USA

⁷Advanced Photon Source, Argonne National Laboratory, Argonne, Illinois 60439, USA

(Received 19 January 2007; revised manuscript received 24 September 2007; published 19 October 2007)

The specific lattice dynamic properties of antimony in the unfilled CoSb_3 and filled $\text{EuFe}_4\text{Sb}_{12}$ skutterudites have been determined by nuclear inelastic scattering at the ^{121}Sb nuclear resonance energy of 37.1298(2) keV with a 4.5 meV high-resolution backscattering sapphire monochromator. The Sb partial vibrational density of states (DOS) shows a maximum centered at 17 and 16 meV in CoSb_3 and $\text{EuFe}_4\text{Sb}_{12}$, respectively. The difference between the Sb DOSs of CoSb_3 and $\text{EuFe}_4\text{Sb}_{12}$ reveals that upon filling there is a transfer of 10% of the vibrational states toward lower energy. Further, a likely indication of the coupling between the guest and the host lattice in rattler systems is observed, a coupling that is required to reduce the lattice thermal conductivity.

DOI: 10.1103/PhysRevB.76.140301

PACS number(s): 63.20.Dj, 78.70.Ck, 76.80.+y

I. INTRODUCTION

The figure of merit of a thermoelectric material is proportional to its electronic conductivity and inversely proportional to its thermal conductivity.¹ Hence, a reduction of the lattice contribution to the thermal conductivity will increase this figure of merit. The rattling motion of the guest R filling the voids in a filled skutterudite such as $RM_4\text{Sb}_{12}$, where R is a rare earth and M is a transition metal,^{1–4} is believed to be an effective way to reduce the thermal conductivity, among others such as mass fluctuation and umklapp scattering.⁵ This hypothesis has led to investigations of the lattice vibrations in both the unfilled CoSb_3 and the filled $RM_4\text{Sb}_{12}$ skutterudites by infrared absorption⁶ and inelastic neutron^{2,4,7–9} and nuclear inelastic^{10–12} scattering.

Both experimental and theoretical studies indicate that the rattling motion of the filling rare earth is essentially harmonic, and hence strongly anharmonic vibrations cannot account for the reduced thermal conductivity of the filled skutterudites.^{2,13} However, purely harmonic Einstein oscillations of the rattler cannot explain the strong phonon scattering and reduced thermal conductivity that filled skutterudites exhibit. Thus hybridization of the rattler and Sb vibrational modes has been proposed,¹³ a hybridization that provides a coupling mechanism of the rattler and the skutterudite framework vibrations. Recently, inelastic neutron scattering by $\text{LaFe}_4\text{Sb}_{12}$ has shown both a deviation from a dispersionless Einstein oscillator model and an important coupling between the La guest and Sb host.⁹

A previous neutron scattering study⁷ indicates that the density of states (DOS) in CoSb_3 consists of three broad peaks between 5 and 25 meV and two narrow peaks between 30 and 35 meV. The analysis of the difference in the inelastic neutron scattering of $\text{La}_{0.9}\text{Fe}_4\text{Sb}_{12}$ and $\text{Ce}_{0.9}\text{Fe}_4\text{Sb}_{12}$ suggests that the major contribution to the peak observed near 12 meV results from the Sb vibrational states⁷ and not from

the rattler, as was also observed in recent measurements and calculations.^{8,9} Because Sb is the common framework element in both the filled and unfilled skutterudites, probing the Sb DOS is crucial both in determining the interactions between the skutterudite framework and the rattler and in understanding how these interactions lead to a reduction in thermal conductivity upon filling. Nuclear inelastic scattering is an element-specific technique for probing lattice vibrations.^{14,15} The first observation of nuclear forward scattering¹⁶ at the 37.1298(2) keV ^{121}Sb resonance makes possible measurements of the nuclear inelastic scattering by Sb.

Herein, we report ^{121}Sb nuclear inelastic scattering measurements on CoSb_3 and $\text{EuFe}_4\text{Sb}_{12}$. These results, combined with those on Fe and Eu,¹⁰ provide a complete experimental determination of the partial DOSs associated with all the elements in $\text{EuFe}_4\text{Sb}_{12}$. The experimental results are compared with earlier theoretical calculations for $\text{LaFe}_4\text{Sb}_{12}$,⁷ and are in good agreement with recent ^{121}Sb nuclear inelastic scattering measurements on $\text{SmFe}_4\text{Sb}_{12}$, for which, however, no DOS was published.¹² The difference between the Sb partial DOSs in CoSb_3 and $\text{EuFe}_4\text{Sb}_{12}$ at ~ 7 meV is likely to correspond to the coupling of the Eu and Sb vibrations.

II. EXPERIMENT

The experiments were performed in 16-bunch mode¹⁷ at the nuclear resonance station ID22N of the European Synchrotron Radiation Facility in Grenoble, France. The experimental arrangement is shown in Fig. 1. A Si (111) high-heat-load monochromator provides the 37.13 keV radiation with a 9 eV bandwidth. A small part of this radiation is then backscattered by the high-resolution monochromator, a sapphire crystal, located in a temperature-controlled nitrogen gas flow cryostat mounted on a four-circle goniometer.¹⁶ Backscattering reduces the spectral bandwidth to a few meV and directs

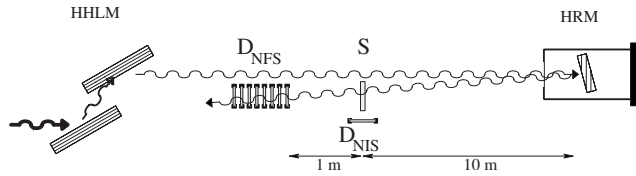


FIG. 1. Schematic view of the experiment, showing the location of the double-crystal Si(111) high-heat-load monochromator (HHLM), the high-resolution monochromator (HRM), which consists of a cooled, temperature-controlled, sapphire single crystal, the ^{121}Sb -containing sample S, and the Si avalanche photodiode x-ray detectors D_{NIS} and D_{NFS} , used to collect the nuclear inelastic and forward scattering by the sample, respectively.

the radiation to the Sb-containing sample. The scattered radiation and the fluorescence products are collected by avalanche photodiode x-ray detectors.¹⁸ The 1 ns resolution of the detectors permits discrimination between the prompt electronically scattered photons and the delayed emitted nuclear fluorescence products.

In order to reach the meV resolution needed for the study of phonon excitations in a solid, a resolution of the monochromator, $\Delta E/E$, of 10^{-7} or better is required. In the present study, a sapphire-based high-resolution Bragg backscattering monochromator has been used.¹⁹ The (15 13 $\bar{28}$ 14) planes of the sapphire crystal satisfy the Bragg backscattering condition in the desired energy region.¹⁶ An angle of 89.92° was used in order to separate the direct and backscattered beams. A linear modulation of the photon energy is obtained by linear temperature scans of the sapphire crystal around $T_0 = 146.54(95)$ K, the temperature corresponding to the energy E_0 of the ^{121}Sb nuclear resonance of 37.1298(2) keV. The variation in the photon energy at this temperature is 59.6 meV/K, and thus a temperature controller with millikelvin accuracy is required. The 12 mg CoSb_3 and $\text{EuFe}_4\text{Sb}_{12}$ absorbers were polycrystalline powders mixed with boron nitride. To minimize multiphonon scattering, both measurements were carried out with the samples at 25 K.

The dependence of the nuclear forward and nuclear inelastic scattering by CoSb_3 and $\text{EuFe}_4\text{Sb}_{12}$ upon photon energy is shown in Fig. 2. The nuclear forward scattering is elastic and yields the resolution function of the sapphire crystal monochromator. The nuclear inelastic scattering corresponds to phonon-assisted scattering. The energy bandwidth of the cryogenic sapphire monochromator was measured to be 4.5 meV in the present experiment, as compared to 7 meV bandwidth measured in Ref. 16. The relative energy resolution is 1.2×10^{-7} . The data analysis, which involves elimination of the multiphonon and background contributions to the scattering, has been carried out with the INES program implemented in IDL code according to Refs. 20 and 21, with 1 meV binning and 50% deconvolution.

III. RESULTS AND DISCUSSION

The Sb DOSs in CoSb_3 and $\text{EuFe}_4\text{Sb}_{12}$, shown in Fig. 3(a), indicate that the Sb vibrational states are found mainly below 30 meV. Both the shape of the DOS and the energy

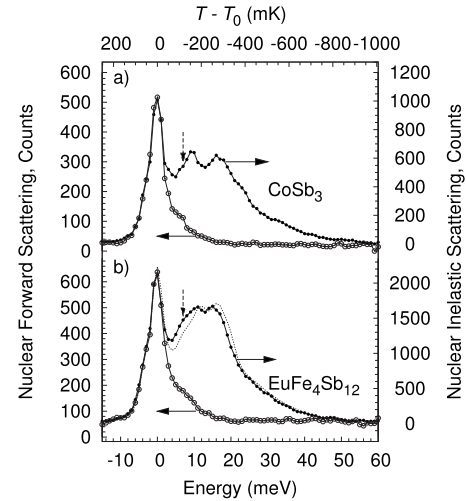


FIG. 2. Temperature-energy dependence of the nuclear forward, open symbols, and nuclear inelastic, closed symbols, scattered intensity from CoSb_3 (a) and $\text{EuFe}_4\text{Sb}_{12}$ (b), with both samples at 25 K. The lines are a guide for the eye. The dashed line in (b) is the calculated nuclear inelastic scattering spectrum with the Sb DOS in $\text{LaFe}_4\text{Sb}_{12}$ (Ref. 7). The temperature $T_0 = 146.54$ K of the sapphire crystal (see upper scale) corresponds to $E_0 = 37.1298(2)$ keV. The dashed arrows indicate the different shape at ~ 7 meV (see text).

range compare well with those measured^{7,9} by inelastic neutron scattering in CoSb_3 , $\text{LaFe}_4\text{Sb}_{12}$, and $\text{CeFe}_4\text{Sb}_{12}$. The present nuclear inelastic measurements permit an unambiguous assignment of the DOS between 7 and 25 meV in the

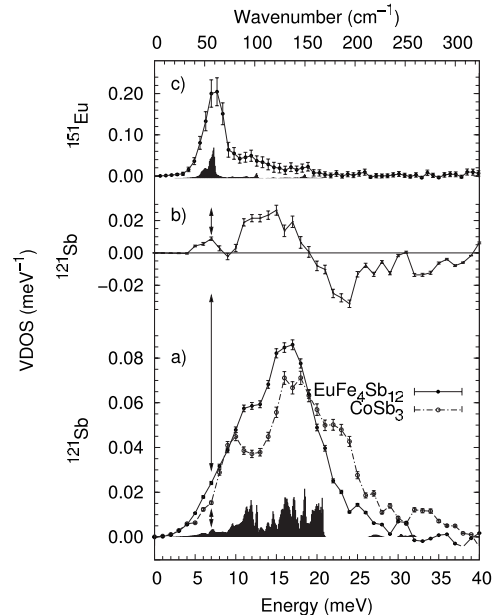


FIG. 3. (a) Sb DOSs in CoSb_3 and $\text{EuFe}_4\text{Sb}_{12}$, and the calculated Sb DOS in $\text{LaFe}_4\text{Sb}_{12}$ (Ref. 7), filled curve; (b) the DOS difference of $\text{EuFe}_4\text{Sb}_{12}$ minus CoSb_3 ; (c) the Eu DOS in $\text{EuFe}_4\text{Sb}_{12}$ (Ref. 10) and the calculated La DOS in $\text{LaFe}_4\text{Sb}_{12}$ (Ref. 7); calculations for $\text{EuFe}_4\text{Sb}_{12}$ are not yet available. The calculated DOSs have been scaled to improve visibility. The arrows emphasize the Eu rattler peak and indicate the likely coupling contribution in the Sb DOS.

TABLE I. The mean force constants Φ , Lamb-Mössbauer factors f_{LM} , and atomic displacement parameters U_{eq} in CoSb_3 and $\text{EuFe}_4\text{Sb}_{12}$.

Compound	Element	T (K)	Φ (N/m)	f_{LM}	U_{eq} (\AA^2)
CoSb_3	Sb	25	117	0.622	0.0013
$\text{EuFe}_4\text{Sb}_{12}$	Sb	25	112	0.607	0.0014
	Eu	25 ^a	35 ^b	0.798	0.0019
	Eu	295 ^a	48 ^b	0.257	0.0114
	Fe	295 ^a	177	0.790	0.0019

^aReference 19.

^b Φ_{Eu} at 25 K was incorrectly reported in Ref. 10 and is corrected here.

inelastic neutron scattering measurements to Sb vibrational states, and provide direct experimental evidence, as shown by the dashed line in Fig. 2(b), in support of the calculated^{7,22,23} partial DOSs, shown in Fig. 3(a), a DOS which is similar to the result of a more recent calculation.⁹ We attribute the 2 meV energy shift between the measured and the calculated spectra to the difference between Eu and La and to the tendency of *ab initio* calculations to obtain a somewhat stiffer lattice than is found experimentally.

A clear minimum is observed near 12 meV in the nuclear inelastic scattering (see Fig. 2). This minimum is much more pronounced in CoSb_3 than in $\text{EuFe}_4\text{Sb}_{12}$, indicating an increased number of Sb vibrational modes in the 12 meV region upon filling. The peak observed in Fig. 3(a) at 10 meV agrees with that observed in the inelastic neutron scattering in CoSb_3 and with that calculated with the model 1 presented in Ref. 7. As is shown in Fig. 3, the Sb DOS in $\text{EuFe}_4\text{Sb}_{12}$ is shifted toward lower energies as compared with CoSb_3 , and 10% of the spectral weight is transferred from above to below 18 meV, as is indicated by the difference in the DOSs [see Fig. 3(b)], a transfer that may be ascribed to a softening of the lattice upon filling.²⁴ This observed shift of the Sb vibrations toward lower frequencies agrees with the trend observed by Raman spectroscopy^{22,25} and with the observation that the process of filling reduces some of the Sb force constants by as much as 30% to 50%.²² The mean force constants obtained herein (see Table I), from the second energy moment of the DOS, are in very good agreement with a theoretical determination²² that found 124, 45, and 172 N/m for Sb, La, and Fe, respectively, in $\text{LaFe}_4\text{Sb}_{12}$. The atomic displacement parameters U_{eq} obtained herein from the Lamb-Mössbauer factor²¹ (see Table I) are generally somewhat lower than those obtained by neutron diffraction,^{26,27} because the atomic displacements of individual nuclei obtained from nuclear inelastic scattering are unaffected by any positional disorder or partial occupancy.

A peak in the difference between the $\text{EuFe}_4\text{Sb}_{12}$ and CoSb_3 DOSs is observed at ~ 7 meV [see Fig. 3(b) and the dashed arrows in Fig. 2], independently of the choice of the binning and deconvolution procedures. Both the composition and the speed of sound differences^{4,24} between $\text{EuFe}_4\text{Sb}_{12}$ and CoSb_3 render a direct interpretation of this peak difficult. We nevertheless interpret this peak as the signature of the coupling of the host Sb phonons with the guest Eu rattler

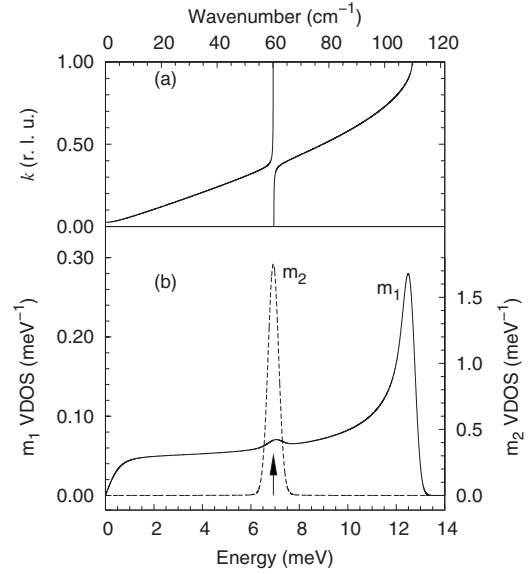


FIG. 4. (a) Dispersion relation in reciprocal lattice units; (b) calculated element-specific DOSs, with a 0.5 meV resolution.

phonons. Support for our interpretation arises from both the peak in the Sb DOS found in the calculated DOS in $\text{LaFe}_4\text{Sb}_{12}$ (Refs. 7 and 9), [see the filled curve in Fig. 3(a)] and the essentially parabolic DOS observed for CoSb_3 below 10 meV.² Further support for our hypothesis comes from a simple Born and Von Karman model of a one-dimensional harmonic chain, with coupling constant κ , connected to a collection of harmonic oscillators, with a force constant λ . This model illustrates that the coupling of the oscillator vibrational modes with the chain vibrational modes leads to a peak in the chain vibrational DOS. The coupling constant between the oscillators and the chain is μ , and the chain and oscillator atoms have masses m_1 and m_2 , respectively. The two differential equations describing such a model,

$$m_1 \ddot{u}_n = -\kappa(2u_n - u_{n-1} - u_{n+1}) - \mu v_n,$$

$$m_2 \ddot{v}_n = -\lambda v_n - \mu u_n,$$

are written in terms of the displacement from the equilibrium position for the n th chain atom, u_n , and the n th oscillator atom, v_n . After the usual ansatz of plane wave solutions,²⁸ i.e., phonon-type solutions which impose a phase relation between chain and oscillator atoms, one obtains a secular determinant $[m_1 \omega^2 - 2\kappa(1 - \cos k\pi)][m_2 \omega^2 - \lambda] = \mu^2$, the solution of which yields the dispersion relation $\omega(k)$ and the DOS $g(\omega) = dk/d\omega$. The simplest representation of the solution is given by the implicit dispersion relation $k(\omega) = \arccos\{1 + [\mu^2/(m_2 \omega^2 - \lambda) - m_1 \omega^2]/2\kappa\}/\pi$.

The DOSs for the specific elements are $g(\omega)/(1+\alpha)$ and $\alpha g(\omega)/(1+\alpha)$ for m_1 and m_2 , respectively, with $\alpha = (\epsilon_2/\epsilon_1)^2 = [\mu/(\lambda - m_2 \omega^2)]^2$ and ϵ_1 and ϵ_2 the oscillation amplitudes for m_1 and m_2 , respectively. In order to compare with the measured element-specific DOSs, the dispersion relation and DOSs in Fig. 4 were calculated with the host mass $m_1 = 1$ and guest mass $m_2 = 1.25$, $\kappa = 40$, $\lambda = 60$, and $\mu = 4$. These values correspond to the mass ratio between Sb and Eu, and yield a

localized mode at 7 meV and a van Hove singularity at 12.5 meV, in agreement with the measured DOS. A small peak in the host DOS is observed under the peak in the guest DOS in Fig. 4. This model indicates that a coupling between the rattler and the host lattice vibrations yields a peak as observed in Fig. 3(b).

We believe that a guest-host coupling peak in the guest DOS is an essential feature of the lattice dynamics in rattler systems, in which the rattlers provide a resonant scattering mechanism. However, such a mechanism is inefficient in lowering the lattice thermal conductivity in the absence of a coupling to the host lattice, the signature of which is observed in our measurements. A likely scenario for the observed⁹ collective rattler phonon mode is thus a coupling of the rattlers through the Sb hosts. A significant lowering of the lattice thermal conductivity has been observed in rattler systems, which illustrates how efficient a resonant mechanism may be, even with weak coupling. Our interpretation also reconciles the calculated,¹³ essentially harmonic, rattler potential with the ability of the rattler to reduce the lattice thermal conductivity.

IV. CONCLUSION

In conclusion, the ¹²¹Sb nuclear inelastic scattering measurements obtained with a 4.5 meV high-resolution sapphire

backscattering monochromator yield the Sb DOSs in the unfilled CoSb₃ and filled EuFe₄Sb₁₂ skutterudites. In conjunction with earlier measurements,¹⁰ the reported measurements provide a complete picture of the element-specific DOSs for all the elements in EuFe₄Sb₁₂. Finally, the difference in the CoSb₃ and filled EuFe₄Sb₁₂ ¹²¹Sb DOSs provides evidence for a weak coupling of the host lattice with the Eu guests, a coupling that is the likely origin of the reduced lattice thermal conductivity in rattler systems.

ACKNOWLEDGMENTS

The authors acknowledge the European Synchrotron Radiation Facility for provision of the synchrotron radiation facilities at beamlines ID18 and ID22N, W. Schweika, H. Schober, and A. I. Chumakov for helpful discussions, and J. Feldman for access to the numerical data of Ref. 7. Part of this research was sponsored by the Division of Materials Sciences and Engineering, Office of Basic Energy Sciences, U.S. Department of Energy, under Contract No. DE-AC05-00OR22725 with Oak Ridge National Laboratory, managed and operated by UT-Battelle, LLC.

*wille@esrf.fr

¹G. A. Slack, *CRC Handbook of Thermoelectrics* (Chemical Rubber Co., Boca Raton, FL, 1995), p. 470.

²R. P. Hermann, R. Jin, W. Schweika, F. Grandjean, D. Mandrus, B. C. Sales, and G. J. Long, *Phys. Rev. Lett.* **90**, 135505 (2003).

³G. A. Slack and V. G. Tsoukala, *J. Appl. Phys.* **76**, 1665 (1994).

⁴V. Keppens, D. Mandrus, B. C. Sales, B. C. Chakoumakos, P. Dai, R. Coldea, M. B. Maple, D. A. Gajewski, E. J. Freeman, and S. Bennington, *Nature (London)* **395**, 876 (1998).

⁵G. S. Nolas, J. L. Cohn, and G. A. Slack, *Phys. Rev. B* **58**, 164 (1998); G. S. Nolas, G. Fowler, and J. Yang, *J. Appl. Phys.* **100**, 043705 (2006).

⁶S. V. Dordevic, N. R. Dilley, E. D. Bauer, D. N. Basov, M. B. Maple, and L. Degiorgi, *Phys. Rev. B* **60**, 11321 (1999).

⁷J. L. Feldman, P. Dai, T. Enck, B. C. Sales, D. Mandrus, and D. J. Singh, *Phys. Rev. B* **73**, 014306 (2006).

⁸R. Vienneis, L. Girard, M. M. Koza, H. Mutka, D. Ravot, F. Terki, S. Charara, and J.-C. Tedenac, *Phys. Chem. Chem. Phys.* **7**, 1617 (2005).

⁹M. M. Koza, M. R. Johnson, R. Vienneis, H. Mutka, L. Girard, and D. Ravot, in *Proceeding of the 25th International Conference on Thermoelectrics, Vienna, 2006* (IEEE-CPMT, Piscataway NJ, 2006), p. 70.

¹⁰G. J. Long, R. P. Hermann, F. Grandjean, E. E. Alp, W. Sturhahn, C. E. Johnson, D. E. Brown, O. Leupold, and R. Rüffer, *Phys. Rev. B* **71**, 140302(R) (2005).

¹¹S. Tsutsui, J. Umemura, H. Kobayashi, Y. Yoda, H. Onodera, H. Sugawara, D. Kikuchi, H. Sato, C. Sekine, and I. Shirogami, *Physica B* **383**, 142 (2006).

¹²S. Tsutsui, Y. Yoda, and H. Kobayashi, *J. Phys. Soc. Jpn.* **76**, 065003 (2007).

¹³J. L. Feldman, D. J. Singh, I. I. Mazin, D. Mandrus, and B. C. Sales, *Phys. Rev. B* **61**, R9209 (2000).

¹⁴M. Seto, Y. Yoda, S. Kikuta, X. W. Zhang, and M. Ando, *Phys. Rev. Lett.* **74**, 3828 (1995).

¹⁵W. Sturhahn, T. S. Toellner, E. E. Alp, X. Zhang, M. Ando, Y. Yoda, S. Kikuta, M. Seto, C. W. Kimball, and B. Dabrowski, *Phys. Rev. Lett.* **74**, 3832 (1995).

¹⁶H.-C. Wille, Yu. V. Shvyd'ko, E. E. Alp, H. D. Rüter, O. Leupold, I. Sergueev, R. Rüffer, A. Barla, and J. P. Sanchez, *Europhys. Lett.* **74**, 170 (2006).

¹⁷R. Rüffer and A. I. Chumakov, *Hyperfine Interact.* **97/98**, 589 (1996).

¹⁸A. Q. R. Baron, *Hyperfine Interact.* **125**, 29 (2000).

¹⁹Yu. V. Shvyd'ko, *X-Ray Optics*, Springer Series in Optical Sciences vol. 98 (Springer, Berlin, 2004).

²⁰V. G. Kohn and A. I. Chumakov, *Hyperfine Interact.* **125**, 205 (2000).

²¹A. I. Chumakov and W. Sturhahn, *Hyperfine Interact.* **123/124**, 781 (1999).

²²J. L. Feldman, D. J. Singh, C. Kendziora, D. Mandrus, and B. C. Sales, *Phys. Rev. B* **68**, 094301 (2003).

²³J. L. Feldman and D. J. Singh, *Phys. Rev. B* **53**, 6273 (1996).

²⁴Y. Luan, S. Bhattacharya, V. Keppens, D. Mandrus, and B. C. Sales, *Bull. Am. Phys. Soc.* **51**(1), R16.9 (2006).

²⁵C. A. Kendziora and G. S. Nolas, in *Thermoelectric Materials 2003—Research and Applications*, edited by George S. Nolas, Jihui Yang, Timothy P. Hogan, and David C. Johnson, MRS Symposia Proceedings No. 793 (Materials Research Society, Pittsburgh, 2004), p. 107.

²⁶M. Puyet, B. Lenoir, A. Dauscher, P. Weisbecker, and S. J. Clarke, *J. Solid State Chem.* **177**, 2138 (2004).

²⁷B. C. Chakoumakos, B. C. Sales, D. Mandrus, and V. Keppens, *Acta Crystallogr., Sect. B: Struct. Sci.* **55**, 341 (1999).

²⁸N. Ashcroft and N. D. Mermin, *Solid State Physics*, 1st ed. (Brooks/Cole Thomson Learning, Belmont, MA, 1976).